



USE OF AN ECR ION SOURCE FOR MASS SPECTROMETRY



D. Button, M.A.C. Hotchkis Australian Nuclear Science and Technology Organisation, Sydney, Australia

Introduction

At ANSTO we have been developing an Isotopic Ratio Mass Spectrometer (IRMS) system utilising an Electron Cyclotron Resonance Ion Source (ECRIS). The ECRIS has two main advantages over traditional systems. Efficient ionization of sample gas upwards of 2 orders of magnitude greater than conventional electron impact ionization, and the brake up of molecules in most cases once ionized greater than 1+ removing molecular interferences. For this reason our IRMS system typically make measurement of the 2+ charge state ions, thus the name adopted for our system is the IRMS++.

Initial testing of the system have proven the ability of the ion source to generate appropriate charge states, and efficient utilisation of the sample. This testing has also found 2 main undesirable characteristics of the ECRIS. These are high backgrounds as shown in Figure 5, and long rise and decay times of samples in the source as demonstrated in Figure 6. Much of our recent work has been focused on suppressing these characteristics, while still maintaining suitable capabilities for IRMS.

Experimental Arrangement

The configuration of the IRMS++ instrument developed at ANSTO is shown in Figure 1, including an electrostatic analyser which has been installed since the work shop report ref[1]. The ECRIS was developed in house to produce low to medium charge state ions with minimal cost. The source is described briefly below: a more detailed description of it can be found in a recent paper [2]. The source operates at 10-25W at a frequency range of 6.85 - 7.15GHz. The magnet field is provided by permanent magnets, constructed from 2 ring magnets to form the axial field, and a hexapole from the radial field. The axial field characteristics can be seen in Figure 7. The plasma chamber is formed by a closed end quartz plasma bottle, and a gold plated plasma facing electrode with a 2.5mm aperture which can also be seen in Figure 7. Gases are delivered via silica capillaries, allowing transfer of gases from the sample chambers at pressures ranging from 5-1000 Torr.

Post extraction, the system incorporates an einzel lens, followed by X and Y steerers. Beams are energy-analysed with the electrostatic analyser and separated according to their mass to charge ratio in the analysing magnet. Multiple beams can be measured simultaneously by the Faraday Cup array. The UHV system is oil free, and regularly achieve base pressures $<4 \times 10^{-9}$ Pa.

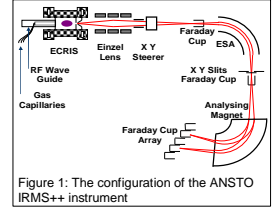


Figure 1: The configuration of the ANSTO IRMS++ instrument

High Backgrounds & Contamination

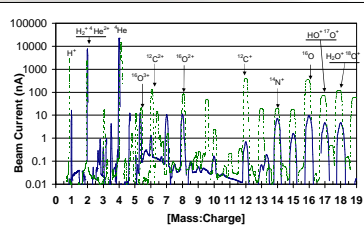


Figure 5: This chart shows in green the mass spectrum of 5N helium before modification and treatment were made, and in blue the resulting spectrum after modifications to the ion source and changes to the cleaning methods.

The Problem:

As the IRMS++ system is intended for the measurement of isotopic ratios of oxygen, carbon, and nitrogen in substances such as water carbon dioxide, nitrogen gas, etc. it is imperative that the residual sources of these species be minimized in the system.

Figure 5 show a typical mass spectrum capture during of 5N purity helium 99.999%. Plotted in green shows the spectrum from the original source configuration which shows the presence of oxygen, hydrogen, and carbon peaks of the order of hundreds of nanoamps compared to just over 10pA of helium beam. The blue plot shows the resulting spectrum after improvements and treatments were made to the ion source.

Sources of Contamination:

The following process were found to contribute the overall background of the ion source.

Source of Contamination	Modification
The original clean procedure was found to still leave surface contamination on the inner surface of the quartz ion source bottle	To complement the cleaning, the quartz bottle is now baked in an atmospheric furnace at 1000°C for 2 hours to burn off surface organics, and carbon. See Figure 2.
Oxygen or water vapour contamination in the helium carrier gas.	A new manifold is under construction, featuring gas specific filters to reduce contaminants below <1ppb levels.
The contaminants in the helium carrier gas were frozen out of the gas stream via a liquid nitrogen trap.	
Outgassing of ferrules used to seal the capillaries	An alternative all metal sealing product for the capillaries namely Siltite [5] ferrules were installed in place of the Vespel system.
Heating of the original Vespel [5] ferrules showed a constant out gassing level suggesting a permeation or leak. Retightening of the ferrule made no impact on this rate.	Baking of these fittings showed a distinctive outgassing cycle with no sign of an ongoing leak, or permeation.
Outgassing or permeation of elastomer (FKM 'Viton') seal used to join stainless steel fittings to quartz inlet tube on the plasma chamber.	To prevent this process the stainless steel fitting was modified and adhered to the quartz with Torr Seal [6] epoxy.
Figure 3 shows the increase in the 16O2+ beam over 16 hours after the wetting of the Viton o-ring.	This gave an improved performance over the elastomer seal and can also be baked to 120°C. After initial baking of the Torr Seal bond and fitting, there is no respond to re-heating the join and fitting.
Oxygen, water, or oxide layers on the inside of the plasma chamber.	Surface cleaning of the ion source was performed by running hydrogen in the plasma.
To establish that these layers are generated by the plasma, the magnet array was displaced, moving the ECR zone and loss zones relative to the plasma bottle. This showed the increase in background levels. After letting the bottle clean up in the displaced position, the magnet array was moved back to the original position, once again the background increased.	Figure 4 (a) and 4 (b) demonstrates the cleaning process of the hydrogen with the decaying 16O2+ beam as the oxygen contamination is cleaned from the plasma chamber.



Figure 2: The top images show residual surface contamination on the plasma electrode and on the plasma bottle. The lower images show the ion source bottle after atmospheric baking at 1000°C for 2 hours. Note that the plasma electrode, and the rear of the plasma bottle both display a clean region which is in line with the loss zone of the plasma and is surrounded by the contaminants.

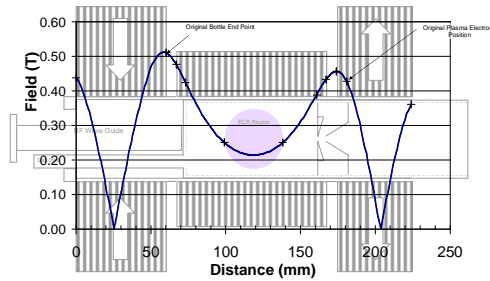


Figure 7: The above is a plot of the axial field of the ECRIS magnet array. The relative positions of the various elements of our ion source are can be seen with respect to the field structure. Note that the plasma facing electrode, and end of the quartz plasma bottle are located on the ECR zone side of their respective B_min.

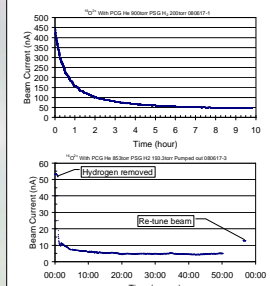


Figure 4: Chart (a) shows the reduction in the 16O2+ beam over a period of 10 hours after the introduction of hydrogen into the ion source. Chart (b) shows the reduction in the 16O2+ over 1 hour after the removal of the hydrogen.

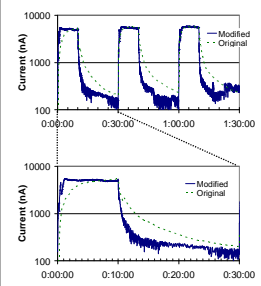


Figure 6: The chart shows the original, and modified ion source rise and decay characteristics of 14N2+ beam over 3 cycles of nitrogen gas introduced for 10 minutes, then pumped away for 20 minutes.

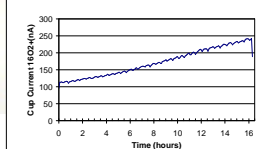


Figure 3: This chart shows the increasing 16O2+ background over 16 hours due to the wetting of the FKM 'Viton' o-ring of the Ultratort fitting. The fitting couples the quartz tube to stainless steel fittings of the ion source sample delivery tube.

Ion Source Retention

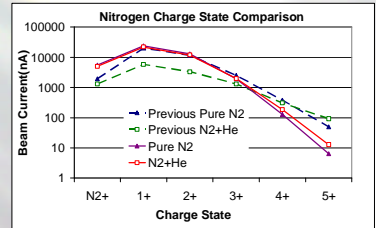


Figure 8: This plot shows the beam current of each of the charge states of nitrogen produced by the ion source with the original and compacted ion source geometries.

The Problem:

Long rise and decay times, or memory effects impacted on the cycle time between samples, and potentially effected the validity of the measurements of isotopic ratios. Figure 6 shows the rise and decay of the 14N2+ beam from the introduction and removal of a nitrogen gas sample. The nitrogen was introduced for 10 minutes and pumped away for the remainder of the 30 minute cycle. The green plot showing the pre-modified results, and in blue the results of modifications made to the ECRIS.

Source Retention Processes:

Our investigations into the rise and decay effects has established the following characteristics.

- The rise & delay effect is not a vacuum conductance effect. This is was proven by the variation of the length of the capillaries that supply the gas to the ion source, and via dummy runs of the gas into the source with the plasma extinguished.
- Inert gases are not retained as strongly as reactive species. The same process used in Figure 6 was performed with Helium, Neon, and Argon. All of these inert gases had a much faster rise and decay rate.
- Surface reactivity of the plasma bottle does not play a strong role in the rise and decay process. The inner cylindrical surface of the quartz plasma bottle was gold plated by evaporation. This showed no impact on the rise and decay rate.
- The process of retaining sample, and releasing sample is performed by the plasma. The plasma was turned off and back on during different parts of the sample cycle, as well as extended periods of time after reaching maximum beam output. Each time the plasma was restarted, the beam current would continue along the same part of the rise or decay cycle at which it was turned off. The presence of sample contamination after restarting the plasma was still present even after being left off for extensive periods.
- The point of delivery of the gas does not effect the retention. A quartz gas delivery tube was installed to deliver the gas axially at the rear edge of the ECR zone of the ion source, as to try and ionize the gas before it contacts the walls of the chamber and confine it in the magnetic field. This showed no effect on the rise or decay rate, but showed we could reduce the plasma chamber size without extinguishing the plasma.

Modifications:

As a consequence of the above characteristics, the ion source chamber was modified so that the plasma facing electrode was placed closer to the ECR zone as was the rear of the plasma bottle. This can be seen in Figure 7.

The consequence of this was that the front and rear mirror ratios were effectively reduced from, 2.10 to 1.81, and 2.40 to 1.98 respectively. This appears to have little impact on our work charge state of 2+ as seen in Figure 8.

The benefits of these modifications can be seen comparably in figure 6, which show that increase in the rate of rise and decay.

References

- [1] M.A.C. Hotchkis, D. Button, C.L. Waring, Rapid Comm. Mass Spectrom. 22 (2008) 1408.
- [2] M.A.C. Hotchkis, Buckley D, Button D. Rev. Sci. Instrum. 79 (2008) 02A304.
- [3] K. S. A. Butcher, Affuddin, P. P.-T. Chen, and T. L. Tansley, phys. stat. sol. (c) 0 (2002) 156.
- [4] Supplied by http://www.discoverysciences.com
- [5] Supplied by SGE http://www.sge.com/
- [6] Supplied by Varian http://www.varianinc.com